Eur. Phys. J. B **57**, 9–14 (2007)
DOI: 10.1140/epjb/e2007-00157-8

THE EUROPEAN PHYSICAL JOURNAL B

Structural parameters and pressure coefficients for $\mathrm{CdS_xTe_{1-x}}$: FP-LAPW calculations

S. Zerroug[1], F. Ali Sahraoui[1], and N. Bouarissa[2,a]

[1] Laboratoire d'optoélectronique et composants, Département de Physique, Université Ferhat Abbas, Sétif 19000, Algeria
[2] Department of Physics, Faculty of Science, King Khalid University, Abha, P.O. Box 9004, Saudi Arabia

Received 4 January 2007 / Received in final form 27 April 2007

Abstract. The structural parameters and hydrostatic pressure coefficients of $\mathrm{CdS}_x\mathrm{Te}_{1-x}$ in the two phases, namely zinc-blende and NaCl as well as the transition pressures from zinc-blende to NaCl structures at various S concentrations are presented. The calculations are performed using the full potential linearized augmented plane wave (FP-LAPW) method within the density functional theory (DFT) in the local density approximation (LDA), and two developed refinements, namely the generalized gradient approximation (GGA) of Perdew et al. for the structural properties and Engel-Vosko for the band structure calculations. Detailed comparisons are made with published experimental and theoretical data and show generally good agreement. The present results regarding the studied quantities for compositions x in the 0–1 range ($0 < x < 1$) and for the NaCl phase are predictions and may serve as a reference for experimental work.

PACS. 71.15.Mb Density functional theory, local density approximation, gradient and other corrections – 71.20.Nr Semiconductor compounds

1 Introduction

The II–VI compound semiconductors have recently received considerable interest from both experimental and theoretical points of view [1]. This is due to their potential technological applications from the blue to the near-ultraviolet spectral region. Among these compounds, the cadmium chalcogenides, namely CdS and CdTe have attracted special attention in recent years [2–11]. CdTe has found important applications in γ-ray detectors, infrared windows, solar cells and other optoelectronic devices [12]. Besides, the CdS/CdTe heterojunction has been shown to exhibit excellent electrical properties in the polycrystalline thin-film CdS/CdTe solar cell [13]. Thin film photovoltaic solar cells based on n-type CdS window layers and p-type CdTe absorber layers have been extensively studied for many years. The formation of an intermediate layer of $\mathrm{CdS}_x\mathrm{Te}_{1-x}$ during cell fabrication is now widely acknowledged [14].

Since the advent of nano-devices, based on semiconductors, the detailed understanding of the behavior of these materials under external influences such as pressure is becoming crucial. Experimental and theoretical interest in pressure dependence of electronic and structural properties of II–VI semiconductors has been growing recently [1,15–19]. This is due in part to the developments of the diamond anvil technique, the extension of the range for optical and X-ray measurements under static pressures [20,21] and the advancement of reliable computational methods for electronic band structure and total energy calculation [22,23]. However, these investigations have been much less intense for II–VI ternary semiconductor alloys and hence a fully consistent picture is still lacking for these materials. At ambient pressure most of the chalcogenides crystallize in either the hexagonal wurtzite or the cubic zincblende structure or both. At high pressures, the generally accepted transition sequence for II–VI semiconductors are zincblende or wurtzite to rocksalt and then to β-Sn phases [8,11,23].

Various computational methods have been applied for the calculation of the electronic band-structure and its related parameters for the II–VI semiconductors and their alloys at normal and high pressure [17–19,24–35]. Unfortunately, with few exceptions, most of these methods are not free of adjustable parameters. In the present study, the FP-LAPW method within the framework of the density functional theory (DFT) with both the LDA and GGA is used to investigate the structural and electronic properties of CdS, CdTe and their mixed crystals $\mathrm{CdS}_x\mathrm{Te}_{1-x}$under different hydrostatic pressures. Results regarding the structural parameters, the transition pressures and the energy band-gaps are reported. Comparison is made, when possible, with experimental data and shows generally satisfactory agreement.

---

[a] e-mail: `N_Bouarissa@yahoo.fr`

2 Computations

The computational details are as follows. The calculations were performed using the full-potential linear augmented plane wave (FP-LAPW) method within the framework of the density functional theory (DFT) [36] as implemented in the WIEN 2K code [37]. We used both the local density approximation (LDA) and the generalized gradient approximation (GGA). The exchange-correlation potential for the structural properties was calculated by the GGA based on Perdew et al. [38] form, while for the electronic properties, the exchange-correlation functional of Engel and Vosko (EV-GGA) [39] was applied. In the FP-LAPW method, the wave function and potential are expanded in spherical harmonic functions inside non-overlapping spheres surrounding the atomic sites (muffin-tin spheres) and a plane wave basis set in the remaining space of the unit cell (interstitial region) is used. In the present calculations, a cubic super cell that is composed of eight atoms (four Cd atoms and four shared out between S and Te) is considered. A super cell with layer wise has been used so as to arrange Te and S atoms at 50% of S content. The effect of the tetragonalization on the calculated parameters is estimated and the tetragonal distortion is given in terms of a c/a ratio that is found to be 1.21 and 1.41 for B_3 and B_1 phases, respectively. A plane wave cut-off of $k_{\max} = 8/R_{MT}$ (where R_{MT} is the smallest muffin-tin radius in the unit cell) was used. The muffin-tin (MT) radii were chosen to be 2.2, 2.2 and 2.3 a.u. for S,Te and Cd, respectively. Meshes of 729, 1000, 343 and 512 special k-points were chosen in the whole Brillouin zone for CdTe zinc-blende type (B3), CdTe NaCl-type (B1), CdS (B3) and CdS (B1) structures, respectively. For $\mathrm{CdS}_x\ \mathrm{Te}_{1-x}$ ternary alloys, 27 and 125 special k-points were chosen for B3 and B1 structures, respectively. Both the plane wave cut-off and the number of k-points were varied to ensure total energy convergence.

3 Results and discussions

CdS and CdTe are characterized by different degrees of covalent, ionic and metallic bonding. At ambient pressure, they crystallize in different crystal structures such as zinc-blende and wurtzite [11]. In the present study, the zinc-blende structure is assumed for both compounds. While for CdTe, the zinc-blende structure is the natural phase, for CdS it is possible to produce thin crystals with the zinc-blende phase for CdS with the molecular-beam epitaxy technique [3,7,8,11]. Both compounds, i.e. CdTe and CdS undergo a transition from zinc-blende to NaCl structure when pressure is applied. Thus, both structures zinc-blende-type (B3) and NaCl-type (B1) have been analyzed for x compositions 0, 0.25, 0.50, 0.75 and 1. The variation of the total energy versus the volume have been calculated for these compounds and as an example, the obtained results for $\mathrm{CdS}_{0.50}\mathrm{Te}_{0.50}$ are plotted in Figure 1 for both phases B3 and B1. In order to determine the equilibrium structural parameters, the curve of Figure 1 has been fitted to the Murnaghan's equation of state. This has been made for all compositions x cited above. In Table 1, we show the LDA and GGA results regarding the equilibrium lattice constant a_0, volume V_0, bulk modulus B_0, and pressure derivative of the bulk modulus B_0' for zinc-blende and NaCl-type structures at zero pressure for the compositions x of interest. Also shown for comparison are the available experimental and previous theoretical data reported in the literature. In view of Table 1, one can note that the a_0 values obtained from the GGA calculations for the zinc-blende structure for both compounds CdTe and CdS are overestimated with respect to the experimental ones [40] whereas those from the LDA calculations are underestimated. This is not surprising, the results are consistent with the general trend of the LDA and GGA approximations [19,42–44]. As compared to previous calculations, the results of Deligoz et al. [11], obtained using ab initio calculations, based on norm-conserving pseudopotentials and density functional theory, seem to be better than the present results and those calculated by other authors [4,9, 41]. Based on the all-electron full-potential (FP) Korringa-Kohn-Rostoker (KKR) Green's function method and using the DFT with the local spin-density approximation (LSDA), Asato et al. [41] reported a value of 6.30 Å for a_0 of CdTe. This value underestimates the experimental one by about 3% and is smaller than all the other theoretical results cited in Table 1. In the absence of experimental and previous theoretical results regarding a_0 at compositions $x = 0.25$, 0.50 and 0.75 for B3 phase as well as at all compositions x for B1 phase, to the best of the author's knowledge, the present results may serve as a reference. The bulk modulus for the B3 phase of both CdTe and CdS compounds as illustrated by the present GGA calculation is in better agreement with the experimental values reported in reference [40] than the previous theoretical data quoted in references [4,9,11]. However, it is worth noting that while the LSDA result for CdTe reported in reference [41] gives a $a_0$value much smaller than the experimental one compared to previous calculations and the present ones, Asato et al. [41] show that with the use of the LSDA, the compared bulk modulus value of CdTe is in excellent agreement with experiment. The same excellent agreement is obtained in our case by the use the LDA calculation. Hence, it could be expected that the LDA would

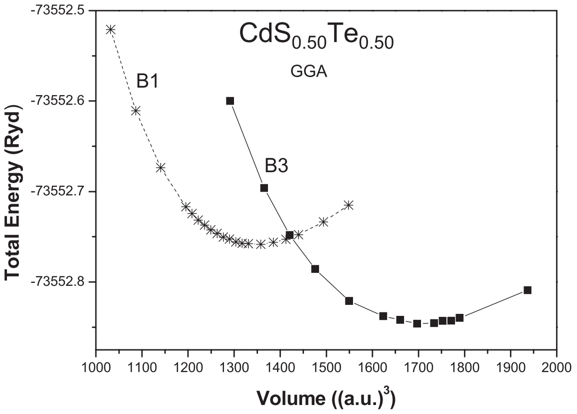

Fig. 1. Total energy versus volume for $\mathrm{CdS}_{0.50}\mathrm{Te}_{0.50}$.

Table 1. Equilibrium lattice constant a_0, bulk modulus B_0, and pressure derivative of B_0 (B_0') for the B3 and B1 phases of CdS$_x$Te$_{1-x}$ at various x compositions.

Composition	a_0 (Å)		B_0 (GPa)		B_0'	
(x)	B3	B1	B3	B1	B3	B1
0	6.41^a	5.94^a	45^a	61^a	4.6^a	4.3^a
	6.62^b	6.11^b	39^b	56^b	3.9^b	3.8^b
	6.48^c		44.5^c		4.47^d	
	6.48^d		48.94^d			
	6.40^e		52^e			
	6.44^f		46.6^f			
	6.30^g		45^g			
0.25	6.28^a	5.81^a	54.8^a	66^a	3.9^a	4.4^a
	6.49^b	5.99^b	38.0^b	56^b	4.3^b	3.9^b
0.50	6.14^a	5.68^a	54.0^a	74^a	4.5^a	4.3^a
	6.33^b	5.86^b	41.6^b	58^b	4.3^b	4.0^b
0.75	5.97^a	5.52^a	59.0^a	84^a	5.0^a	4.3^a
	6.15^b	5.69^b	47.0^b	65^b	4.4^b	4.1^b
1	5.77^a	5.35^a	70.0^a	94^a	4.8^a	4.3^a
	5.94^b	5.51^b	55.8^b	75^b	4.3^b	3.9^b
	5.82^c		62^c		4.31^d	
	5.81^d		72.42^d			
	5.85^e		70^e			
	5.80^f		70.3^f			

[a] Present work: LDA; [b] Present work: GGA; [c] experiment [40]; [d] theory [11]; [e] theory [4]; [f] theory [9]; [g] theory [41].

improve the results of the bulk modulus values for different x S contents in CdS$_x$ Te$_{1-x}$. So far, to the best of our knowledge, no experimental or theoretical data have been reported regarding the bulk modulus of B1 phase at all x compositions and for B3 for the compositions x other than 0 and 1; hence once again the present results are predictions. Because of the lack of experimental data regarding B_0' for both B3 and B1 phases, the present LDA and GGA results are compared with the recent theoretical investigations reported by Deligoz et al. [11] for the B3 phase. These comparisons reveal that the present GGA value of B_0' agrees very well with that of reference [11] for CdS compound, while for CdTe it is somewhat smaller. However for the present LDA results, when compared to the values reported in reference [11], one can note good agreement for CdTe and an overestimation of B_0' for CdS. Note that as one goes from $x = 0$ (CdTe) to $x = 1$ (CdS), the bulk modulus increases non-monotonically from 38.58 to 55.76 GPa for the B3 phase, and monotonically from 55.48 to 74.97 GPa for the B1 phase. This suggests that as x increases from $x = 0$ (CdTe) to $x = 1$ (CdS), CdS$_x$Te$_{1-x}$ becomes generally less compressible.

The transition pressures (p_t) between zinc-blende (B3 phase) to NaCl (B1 phase) of CdS$_x$Te$_{1-x}$ at various x compositions ranging from 0 to 1 were determined by calculating the Gibbs free energy (G), ($G = E_0 + PV - TS$) for these two phases. Since the present calculations are performed at $T = 0$ K, the Gibbs free energy becomes equal to the enthalpy i.e. $H = E_0 + PV$. In Figure 2, the enthalpy H has been plotted against the pressure up to 60 GPa for CdS$_{0.50}$Te$_{0.50}$ and for both phases. The two H vs. pressure curves corresponding to the B3 and B1 phases cross at a pressure of 3.75 GPa suggesting therefore that the transition pressure (p_t) from B3 to B1 is 3.75 GPa. Following such a procedure, the zinc-blende to NaCl transition pressures were calculated for CdS$_x$Te$_{1-x}$ at various x compositions. The obtained results are listed in Table 2, along with the available experimental and theoretical data from the literature. According to our LDA and GGA results, the CdTe zinc-blende phase transforms to the NaCl one at 2.53 and 3.99 GPa, respectively. The agreement between our GGA value and that reported by Mariano and Warekois [45] is better than 15%. No comparison has been made for p_t of CdS$_x$Te$_{1-x}$ in the $0 < x \leqslant 1$ composition range, since to the best of our knowledge there are no known available data. Hence, the present transition pressure values p_t in this composition range are predictions. One should also note that when going from the composition $x = 0$ to $x = 1$, the variation of p_t is non-monotonic. The transition pressure from the zinc-blende to the NaCl structures for CdS as derived by our LDA and GGA results is respectively 2.03 and 2.68 GPa. The GGA result gives better agreement with experiment [46,47] than the LDA one.

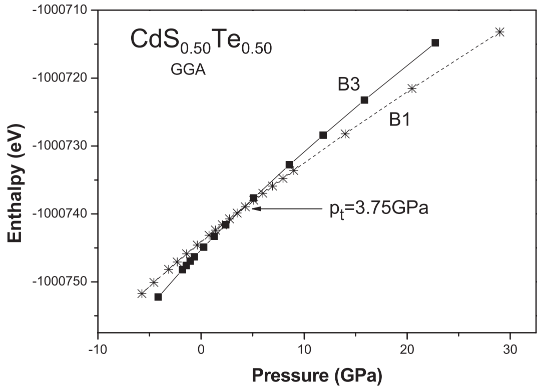

Fig. 2. Enthalpy versus pressure for CdS$_{0.50}$Te$_{0.50}$.

Table 2. Transition pressures (p_t) for the zinc-blende to the NaCl structures for CdS$_x$Te$_{1-x}$ at various x compositions.

Composition (x)	p_t(GPa)
0	2.53 ^{a}; 3.99^b; 3.5^c; 2.8^d
0.25	2.30^a; 3.19^b
0.50	2.03^a; 3.75^b
0.75	2.00^a ; 3.95^b
1	2.03^a; 2.68^b; 2.5^d; 3.1^e

[a] Present work: LDA; [b] present work: GGA; theory: [c] reference [45]; experiment: [d] reference [46]; [e] reference [47].

We now turn our attention to the electronic properties, such as the direct and indirect energy band-gaps and their composition and pressure dependence. For this purpose, the band structure of CdS$_x$Te$_{1-x}$ were obtained in the B3 phase within the EV-GGA scheme at ambient and high pressures for different x compositions ranging from 0 to 1. Figure 3. shows the variation of the fundamental band-gap energy ($\Gamma - \Gamma$) in CdS$_x$Te$_{1-x}$ as a function of x under different pressures ranging from 0 up to 3 GPa. It can be

Table 3. Calculated linear pressure coefficients of the direct and indirect band-gaps (in eV/GPa) for CdS_xTe_{1-x} at various x compositions.

Composition (x)	Pressure coefficients		
	$\frac{dE_{\Gamma\Gamma}}{dp}$	$\frac{dE_{\Gamma X}}{dp}$	$\frac{dE_{\Gamma L}}{dp}$
0	0.081[a]; 0.065[b] 0.0839[c]; 0.114 0.08[e]; 0.028[f] 0.063[g]	0.014[a]; −0.043[f] −0.0448[g]	0.033[a]; 0.005[f] 0.021[g]
0.25	0.077[a]	0.073[a]	0.057[a]
0.50	0.062[a]	0.065[a]	0.052[a]
0.75	0.06[a]	0.073[a]	0.056[a]
1	0.05[a]; 0.0285[c] 0.03[g]; 0.046[h]	−0.015[a]; −0.023[g]	0.037[a]; 0.0196[g]

[a] Present work: EV-GGA; [b] experiment [52]; [c] theory [11]; [d] theory [53]; [e] experiment [54]; [f] theory [54]; [g] theory [16]; [h] experiment [55].

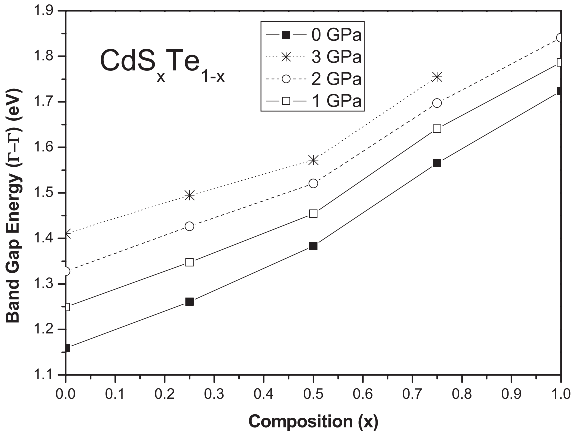

Fig. 3. Fundamental band-gap energy $(\Gamma-\Gamma)$ versus x composition for zinc-blende CdS_xTe_{1-x} at various pressures.

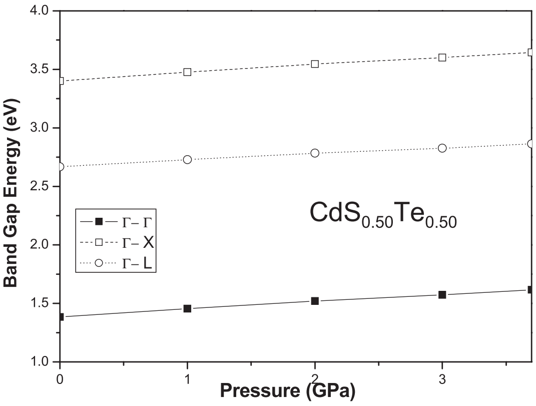

Fig. 4. Direct $(\Gamma-\Gamma)$ and indirect $(\Gamma-X)$ and $(\Gamma-L)$ band-gap energies versus pressure for $CdS_{0.50}Te_{0.50}$.

clearly seen, in Figure 3, that the direct band-gaps $(\Gamma-\Gamma)$ for CdTe ($x=0$) and CdS ($x=1$) are still underestimated compared to the experimental values which are 1.60 [48] and 2.55 eV [40] for CdTe and CdS, respectively. However, our result for the energy-gap of CdTe obtained within EV-GGA formalism shows better agreement with experiment than the theoretical value (0.82 eV) reported by Poon et al. [48] using ab initio self-consistent pseudopotential method with spin-orbit correction. It is well-known that the GGA usually underestimates the experimental energy band-gap [19,42]. The GGA has a simple form which is not sufficiently flexible for accurately reproducing both exchange-correlation energy and its charge derivative [19]. Engel and Vosko [39] by considering this shortcoming constructed a new functional form of the GGA which was able to better reproduce the exchange potential at the expense of less agreement as regards exchange energy when compared to experiment, This approach, called the EV-GGA, yields better band-gap energies compared to the GGA. This is consistent with the results reported by Charifi et al. [19] on calcium chalcogenides. One can also note that the direct band-gap $(\Gamma-\Gamma)$ increases with increasing the S content. This could be understood in terms of the difference in the electro-negativity between Te and S atoms which is according to the Pauling scale 2.58 for S and 2.1 for Te. This behavior appears to be independent of the applied pressure. As pressure is increased, the $(\Gamma-\Gamma)$ band-gap increases in magnitude at each x composition.

The linear pressure coefficients are important parameters for fundamental research and device applications. Applied high pressure thoroughly probes the physics of interatomic bonding extremely and thus changes the physical properties of semiconductors. The interatomic distance decreases under applied pressure and usually the direct band-gap $(\Gamma-\Gamma)$ increases [49–51]. The pressure dependence of the direct $(\Gamma-\Gamma)$ and indirect $(\Gamma-X)$ and $(\Gamma-L)$ band-gap energies was studied for various S contents in zinc-blende CdS_xTe_{1-x} mixed crystals with x-composition increments of 0.25. As an example, the obtained results calculated using the EV-GGA for the equimolar alloy $CdS_{0.50}Te_{0.50}$ are shown in Figure 4. The calculated linear pressure coefficients of the direct and indirect band-gaps for zinc-blende CdS_xTe_{1-x} mixed crystals at various x compositions are given in Table 3, along with the experimental and previous theoretical data which are available only for the parent compounds, i.e. CdS and CdTe. From Figure 4, one can note that as pressure increases all studied band-gap energies linearly increase. This behavior is similar to that reported for III-V [49–51] and other II–VI [11] semiconductors. Also the equimolar alloy $CdS_{0.50}Te_{0.50}$ remains a direct band-gap over the pressure range from 0 up to 3.75 GPa as clearly seen in Figure 4. The trend for the pressure dependence of the band-gaps allowed us to deduce the pressure coefficients shown in Table 3. For CdTe, one can note that, the present result (see Tab. 3) regarding the linear pressure coefficient of $\Gamma - \Gamma$ is in excellent agreement with the experimental value cited by reference [54] as well as with that reported by Deligoz et al. [11] using ab initio calculations based on norm-conserving pseudopotentials and DFT. Moreover, our value is closer to the experimental one [54] than that of previous calculations reported in references [16,53,54]. For the linear pressure coefficient of $\Gamma - L$, our result for CdTe is closer to that reported by Wei and Zunger [16] computed within the LDA than that reported by Tsay et al. [54] using the empirical pseudopotential method. However, for $\Gamma - X$, the linear pressure coefficient of CdTe calculated in the present study disagrees with theoretical values reported in references [16,54] in both magnitude and sign. The situation seems to be different for CdS where one notice a reasonable agreement between the present results and those reported in reference [16] for regards the linear pressure coefficients of indirect band gaps $\Gamma - X$ and $\Gamma - L$. However, for the linear pressure coefficient of the direct band gap $\Gamma - \Gamma$ of CdS, our result is larger than those reported in references [11,16] but agrees very well with the experimental value quoted by reference [55]. Again, the present calculated linear pressure coefficients of band-gaps for CdS_xTe_{1-x} $(0 < x < 1)$ are predictions. It is worth noting that the linear pressure coefficient of the direct band-gap $\Gamma - \Gamma$ decreases when going from CdTe to CdS. Very recently, Deligoz et al. [11] reported that there is a relation between mass and linear pressure coefficient. According to the present results, this relation consists on the fact that when the mass between Cd and an element of group VI increases, the linear pressure coefficient of $\Gamma - \Gamma$ band-gap increases as well. This is consistent with the results of Deligoz et al. [11] obtained for cadmium chalcogenides and those of Charifi et al. [19] obtained for calcium chalcogenides.

4 Conclusion

FP-LAPW method within the DFT in the LDA and GGA. for structural properties and EV-GGA for electronic band structure have been used to calculate structural parameters, hydrostatic pressure coefficients and transition pressures of CdS_xTe_{1-x} mixed crystals $(0 \leqslant x \leqslant 1)$ in the two phases, zinc-blende and NaCl. A summary of the key findings follows.

(i) The calculated lattice parameters in the zinc-blende phase, using the GGA sheme, are somewhat overestimated with respect to experiment, while the bulk modulus values are in better agreement with experiment than earlier theoretical calculations.

(ii) As the S content increases, CdS_xTe_{1-x} becomes generally less compressible.

(iii) It is found that the transition pressure from the zinc-blende to the NaCl structures for CdTe is in reasonable agreement with previously obtained one and its variation with the S concentration is non-monotonic.

(iv) The fundamental direct band gap $(\Gamma - \Gamma)$ increases with increasing S concentration.

(v) Applied hydrostatic pressure leads to a linear increase of the energy band-gaps of interest, i.e. $\Gamma - \Gamma$, $\Gamma - X$ and $\Gamma - L$ (except may be $\Gamma - X$ of CdTe and CdS). This allowed the determination of the linear pressure coefficients of the direct and indirect band-gaps of CdS_xTe_{1-x} at various S concentrations. The values of these pressure coefficients are closer to the experimental ones than the previous calculations.

While the present results derived for different S contents 0–1 range $(0 < x < 1)$ and for the NaCl phase are predictions, it is hoped that this work will encourage additional experiments and theoretical investigations on structural and electronic properties of CdS_xTe_{1-x}, especially for the NaCl structure.

We would like to thank Professor A. Layadi for a careful reading of the manuscript, as well as Dr. F. El Haj Hassan and Mr. M. Kharoubi for providing numerical support.

References

1. *Wide Band-gap Semiconductors*, edited by C.G. Van der Walle (North Holland, Amsterdam, 1993); also published as Physica B **185**, 1 (1993)
2. A.D. Corsa, S. Baroni, R. Resta, S. Gironcoli, Phys. Rev. B **47**, 3588 (1993)
3. Y.D. Kim, M.V. Klein, S.F. Ren, Y.C. Chen, H. Lou, N. Samarth, J.K. Furdyna, Phys. Rev. B **49**, 7262 (1994)
4. O. Zakharov, A. Rubio, X. Blase, M.L. Cohen, S.G. Louie, Phys. Rev. B **50**, 10780 (1994)
5. A. Tomasulo, M.V. Ramakrishna, J. Chem. Phys. **105**, 3612 (1996)
6. B.D. Rajput, D.A. Browne, Phys. Rev. B **53**, 9052 (1996)
7. M. Cote, O. Zakharov, A. Rubio, M.L. Cohen, Phys. Rev. B **55**, 13025 (1997)
8. R.J. Nelmes, M.I. McMohan, Semicond. Semimater. **54**, 145 (1998)
9. S. Wei, S.B. Zhang, Phys. Rev. B **62**, 6944 (2000)
10. R. Wright, J. Gale, Phys. Rev. B **70**, 035211 (2004)
11. E. Deligoz, K. Colakoglu, Y. Ciftci, Physica B **373**, 124 (2006)
12. E. Menendez-Proupin, G. Gutierrez, E. Palmero, J.L. Pena, Phys. Rev. B **70**, 035112 (2004)
13. A. Fischer, Z. Feng, E. Bykov, G. Contreras-Puente, A. Compaan, F. de Landa Castillo-Alvarado, J. Avendano, A. Mason, Appl. Phys. Lett. **70**, 3239 (1997)
14. D.W. Lane, Solar Energy Mater. Solar Cells **90**, 1169 (2006)
15. O. Zakharov, A. Rubio, M.L. Cohen, Phys. Rev. B **51**, 4926 (1995)
16. S.-H. Wei, A. Zunger, Phys. Rev. B **60**, 5404 (1999)

17. F. Benmakhlouf, A. Bechiri, N. Bouarissa, Solid State Electron. **47**, 1335 (2003)
18. F. Benmakhlouf, N. Bouarissa, Intern. J. Modern. Phys. B **20**, 4807 (2006)
19. Z. Charifi, H. Baaziz, F. El Haj Hassan, N. Bouarissa, J. Phys.: Condens. Matter **17**, 4083 (2005)
20. W.B. Holzapfel, Rep. Prog. Phys. **59**, 29 (1996)
21. J.V. Badding, Annu. Rev. Mater. Sci. **28**, 631 (1998), and references therein
22. G.J. Ackland, Rep. Prog. Phys. **64**, 483 (2001), and references therein
23. A. Mujica, A. Rubio, A. Munoz, R.J. Needs, Rev. Modern Phys. **75**, 863 (2003)
24. J.A. Van Vechten, T.K. Bergstresser, Phys. Rev. B **1**, 3351 (1970)
25. D.J. Chadi, Phys. Rev. B **16**, 790 (1977)
26. P.A. Feldders, C.W. Myles, Phys. Rev. B **29**, 802 (1984)
27. A. Baldereschi, E. Hess, K. Maschke, H. Neumann, K.R. Shulze, K. Unger, J. Phys. C **10**, 4709 (1977)
28. Y.P. Feng, K.L. Teo, M.F. Li, H.C. Poon, C.K. Ong, J.B. Xia, J. Appl. Phys. **74**, 3948 (1993)
29. Z. Charifi, H. Baaziz, N. Bouarissa, Physica B **337**, 363 (2003)
30. Z. Charifi, H. Baaziz, N. Bouarissa, Mater. Chem. Phys. **84**, 273 (2004)
31. J.E. Bernard, A. Zunger, Phys. Rev. B **36**, 3199 (1987)
32. S.H. Wei, A. Zunger, Phys. Rev. B **43**, 1662 (1991)
33. K. Kassali, N. Bouarissa, Mater. Chem. Phys. **76**, 255 (2002)
34. S. Ben Afia, H. Belmabrouk, M. Said, S. Abdi-Ben Nasrallah, N. Bouarissa, Mater. Sci. Eng. C **25**, 691 (2005)
35. S. Abdi-Ben Nasrallah, N. Sfina, N. Bouarissa, M. Said, J. Phys.: Condens. Matter **18**, 3005 (2006)
36. P. Hohenberg, W. Kohn, Phys. Rev. B **136**, 864 (1964)
37. P. Blaha, K. Schwarz, G.K.H. Madsen, D. Kvasnicka, J. Luitz, *WIEN 2K, An Augmented Plane Wave + Local Orbitals Program for Calculating Crystal Properties*, edited by Karlheinz Schwarz (Techn. Universitat, Wien, Austria, 2001)
38. J.P. Perdew, S. Burke, M. Ernzerhof, Phys. Rev. Lett. **77**, 3865 (1996)
39. E. Engel, S.H. Vosko, Phys. Rev. B **47**, 13164 (1993)
40. *Numerical Data and Functional Relationships in Science and Technology*, edited by O. Madelung, M. Schulz, H. Weiss, Landolt-Borstein (Springer, Berlin, 1982), Vol. 17
41. M. Asato, A. Settels, T. Hoshino, T. Asada, S. Blugel, R. Zeller, P.H. Dederichs, Phys. Rev. B **60**, 5202 (1999)
42. S. Saib, N. Bouarissa, Solid State Electron. **50**, 763 (2006)
43. F. El Haj Hassen, H.Akbarzadeh, S.J. Hashemifar, A. Mokhtari, J. Phys. Chem. Solids **65**, 1871 (2004)
44. S. Saib, N. Bouarissa, Phys. Stat. Sol. B **244**, 1063 (2007)
45. A.N. Mariano, E.P. Warekois, Science **142**, 672 (1963)
46. J.E. Jaffe, R. Pandey, A.B. Kunz, Phys. Rev. B **43**, 14030 (1991)
47. M. Haase, A.P. Alivisatos, J. Phys. Chem. **96**, 6756 (1992)
48. H.C. Poon, Z.C. Feng, Y.P. Feng, M.F. Li, J. Phys.: Condens. Matter **7** 2783 (1995)
49. N. Bouarissa, Phys. Stat. Sol. B **231**, 391 (2002)
50. N. Bouarissa, Europ. Phys. J. B **26**, 153 (2002)
51. M. Boucenna, N. Bouarissa, Mater. Chem. Phys. **84**, 375 (2004)
52. D.J. Dunstan, B. Gil, K.P. Homewood, Phys. Rev. B **38**, 7862 (1982)
53. D.G. Thomas, J. Appl. Phys. **32**, 2298 (1961)
54. Y.F. Tsay, S.S. Mitra, B. Bendow, Phys. Rev. B **10**, 1476 (1974)
55. K. Reimann, M. Haselhoff, St. Rubenacke, M. Steube, Phys. Stat. Sol. B **198**, 71 (1996)